Optical and Quantum Electronics **35:** 521–532, 2003.

High brightness 735 nm tapered lasers – optimisation of the laser geometry

B. SUMPF*, R. HÜLSEWEDE, G. ERBERT, C. DZIONK, J. FRICKE, A. KNAUER, W. PITTROFF, P. RESSEL, J. SEBASTIAN AND G. TRÄNKLE

Ferdinand-Braun-Institut für Höchstfrequenztechnik, Abteilung Optoelektronik, Albert-Einstein-Straße 11, D-12489 Berlin, Germany

*(*author for correspondence: E-mail: sumpf@fbh-berlin.de)*

Abstract. High brightness tapered laser diodes with different resonator geometries were fabricated and analysed. The devices consist of an index-guided straight section and a gain-guided tapered section. Lasers with a total length $L = 2$ and 4 mm and different length of the ridge waveguide L_{RW} (500 μm ≤ L_{RW} ≤ 1250 μm for $L = 2$ mm and 500 μm ≤ L_{RW} ≤ 2000 μm for $L = 4$ mm) were processed to study the influence of the straight section on the spatial mode filtering. The power–voltage–current-characteristics, the beam waist, the far field, and the beam propagation factor M^2 were measured. From the experiments, it can be stated that the lasers with a small L_{RW} reach higher output powers compared to those with larger L_{RW}. Concerning the beam quality the length L_{RW} should exceed a minimal value to guarantee efficient spatial mode filtering. Devices optimised concerning maximum output power and excellent beam quality reach a beam propagation factor smaller than 2.1 at an output power $P = 2$ W.

Key words: high brightness lasers, high power diode lasers, tapered lasers, visible lasers

1. Introduction

While high power broad area (BA) lasers with output powers up to several Watts are state of the art; these devices suffer from a bad beam quality. Especially, for applications requiring fibre coupling, high brightness sources, i.e. sources with high power in a small divergence angle are under development. The requirement of high brightness corresponds to nearly diffraction-limited beams with a small beam propagation factor M^2.

The interest in high brightness diode lasers for the spectral wavelength range around 735 nm originates by at least two types of applications:

- Photodynamic therapy (PDT) in the range 720 nm ≤ λ ≤ 760 nm and
- Pumping of solid-state lasers.

High power BA diode lasers with an AlGaAs quantum well (QW) were reported by Tihanyi *et al.* (1994). These lasers reached an output power up to 540 mW at 715 nm. This output power could be increased to 2.2 W by Emanuel *et al.* (1997) by applying a single InAlGaAs QW. Singh *et al.* (1999) presented 100 μm stripe width BA laser diodes based on an AlGaAs triple

quantum wells (TQW). These devices exhibit reliable operation over 1000 h at 1 W and 20°C. Aluminium free compressively strained InGaAsP QW's were used by Bour *et al.* (1994) and Al-Muhanna *et al.* (1998a). Reliable operation at 1 W and 25°C up to 950 h could be demonstrated (Al-Muhanna *et al.* 1998b; Rusli *et al.* 2000).

Agahi *et al.* (1995, 1997) reported the application of tensile-strained GaAsP QWs embedded in AlGaAs for diode lasers near 770 nm. Similar structures for the wavelength range between 715 and 785 nm were manufactured in our group (Erbert *et al.* 1999). For a laser with 100 μm aperture and 2000 μm lengths an output power of 7 W could be reported in Knauer *et al.* (1999). Reliable operation near 735 nm with degradation rates below $5 \times 10^{-5}\ \mathrm{h}^{-1}$ at 2 W output power over more than 2000 h (Sumpf *et al.* 2001a, b) was achieved.

These BA devices with a stripe width of about 100 μm suffer from a poor beam quality. Typical beam divergences ($1/e^2$-values) are at least 10 times larger than the diffraction limit, i.e. $M^2 > 10$.

To improve the beam quality, tapered lasers were developed. The devices consist of a straight index-guided section formed by a ridge waveguide (RW) and a gain-guided tapered section. The optimisation of the beam parameters was carried out mainly by optimising the lateral device geometry. This include the following parameters:

- the length of the RW section L_{RW},
- the effective index step in the RW section Δn,
- the taper angle φ_{TR}, and
- the total laser length L.

Previous works by Walpole (1996), Kintzer *et al.* (1993) (980 nm, 1.05 diffraction limited beam profile at 3 W), Mikulla *et al.* (1998) (1020 nm, $M^2 = 3$ at 2.5 W), and Donelly *et al.* (1998) (1500 nm) used tapered lasers with a total length $L \approx 2 \ldots 3$ mm and a total taper angle of $\varphi_{\mathrm{TR}} \approx 6°$. While the taper angle is the same and the total length is very similar in these studies the length of the straight section varies between only 50 μm (Kintzer *et al.* 1993) and 1000 μm (Donelly 1998). This work focuses on the optimisation of the length of the RW section with the goal of high output power together with a high brightness. For two different laser lengths $L = 2$ and 4 mm an identical effective index step, and a constant full taper angle $\varphi_{\mathrm{TR}} = 4°$ the length of the straight section L_{RW} was varied. For the 2 mm long devices L_{RW} was 500, 750, 1000 and 1250 μm. In the case of the 4 mm long lasers L_{RW} was 500, 1000, 1500 and 2000 μm. For above-mentioned geometries the power–voltage–current characteristics and the beam parameters will be presented. Output powers larger than 2 W were measured. For lasers with an optimal geometry a beam propagation factor $M^2 = 2.1$ was found. These investigations led to optimised structures allowing record values for tapered lasers for 735 nm recently reported by our group (Sumpf *et al.* 2002).

2. Laser Structure

The laser structure is similar to that presented in Erbert *et al.* (1999) with a 9 mm thick $GaAs_{0.67}P_{0.33}$ QW embedded in $Al_{0.65}Ga_{0.35}As$ waveguide and $Al_{0.70}Ga_{0.30}As$ cladding layers.

This large optical cavity (LOC) structure has excellent material parameters with an internal efficiency $\eta_i \approx 0.8$, internal losses α_i below 1 cm^{-1}, and a transparency current density $j_{tr} \leq 220$ A/cm^2 (Erbert *et al.* 1999). The typical data for BA devices (100 μm × 2 mm) with antireflection coated front facets ($R_f \approx 3\%$) and high reflectivity coated rear facets ($R_r \approx 95\%$) can be compiled as follows: threshold current density $j_{th} < 250$ A/cm^2, slope efficiency $S = 1.1 \ldots 1.2$ W/A, characteristic temperature of the threshold current $T_0 = 60$ K, wall-plug efficiency of about 50%, and high reliability with a measured lifetime larger than 2000 h at 25°C and 2 W (Sumpf *et al.* 2001b).

The tapered lasers consist of an index-guided straight section and a gain-guided tapered section. The index guiding is achieved by a RW with a width $W_{RW} = 3$ μm.

In order to keep the processing of the lasers as simple as possible no cavity-spoiling grooves for additional transverse-mode filtering were used. The tapered section was manufactured as low mesa-structure. In all experiments described in this paper a full taper angle of 4° was selected.

The metallisation on the p-side contact was formed by evaporating a Ti–Pt–Au multilayer and by electro-plating a thick Au layer. After thinning and n-metallisation the wafer was cleaved to obtain total cavity lengths of $L = 2$ mm and $L = 4$ mm, respectively.

In the experiments described in this paper the facet coating was kept constant. The front facet was antireflection coated ($R_f \approx 1\%$) whereas the rear facet was high-reflection coated ($R_r \approx 95\%$). The devices were mounted p-side (epi-side) down on TcBN heat spreaders in the case of the 2 mm long lasers; for the 4 mm long devices CuW submounts were used. All devices were soldered with AuSn using a procedure previously described for BA lasers (Pittroff *et al.* 2001). The n-side was contacted by wire bonding.

3. Characteristics of 2 mm long devices

Typical power–current characteristics for 2 mm long devices with different length of the RW section L_{RW} are shown in Fig. 1. The corresponding threshold currents and slope efficiencies are compiled in Table 1. It is obvious that the lasers with a smaller L_{RW} have higher threshold currents due to the larger area of the tapered section. The lasers with $L_{RW} = 500$ and 750 μm have slope efficiencies $S \geq 1.0$ W/A and reach an output power of 2.4 W at a current $I = 3$ A. For both diodes wall-plug efficiencies of about 45% were

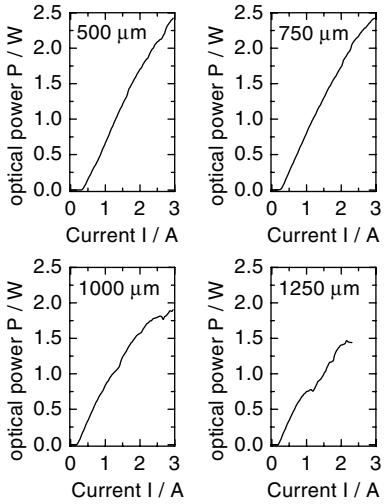

Fig. 1. Power–current characteristics for four tapered diode lasers with a laser length $L = 2$ mm and different length of the RW L_{RW}. The other geometrical parameters are $\varphi_{TR} = 4°$ and $W_{RW} = 3$ µm. The measurement temperature was $T = 25°C$.

Table 1. Electro-optical parameter for tapered laser with a total length $L = 2$ mm and different L_{RW}

L_{RW} (µm)	I_{th} (mA)	S (W/A)	I_{max} (A)	P_{max} (I_{max}) (W)
500	347	1.1	3.0	2.4
750	272	1.0	3.0	2.4
1000	194	0.6	3.0	1.9
1250	192	0.6	2.3	1.4

measured. The devices with a ridge length $L_{RW} \geq 1000$ µm have smaller threshold currents, remarkably lower slope efficiencies, and some kinks in the power–current dependence. The maximum output power is limited to about 1.9 W at $L_{RW} = 1000$ µm and 1.4 W at $L_{RW} = 1250$ µm. Moreover, the maximum current for the device with $L_{RW} = 1250$ µm is limited to about 2 A; at higher current the lasers were destroyed.

To evaluate the beam quality of the tapered lasers, the beam propagation factor M^2 was determined. For this purpose, the position of the beam waist and the intensity profiles in the beam waist and in the far-field for the slow axis were measured applying the method of the moving slit (DIN/ISO 11146, Annex A).

The measurement of the far-field pattern was done by using a high aperture lens combination. This system converts the angular distribution of the divergent laser beam into a spatial distribution at the plane of the moving slit. With the used set-up an angular resolution of about 0.01° can be achieved.

The intensity profile of the beam waist was measured by magnifying the waist by a factor 40 with a telescope. The spatial resolution was limited to

about 2 μm. The transmitted intensity of the laser was detected by a large area pin-diode.

The position of the beam waist inside the laser was determined with the help of a CCD-camera system. The distance between the first lens of the telescope and the laser was reduced until a sharp image of the beam waist was monitored with the CCD-system. The difference in the lens position used for the far-field measurement and the beam waist measurement is equal to the astigmatism of the tapered laser.

From the measured intensity profiles of the far-field and the beam waist, the beam propagation factor M^2 was calculated. The beam widths needed to calculate M^2 were identified with the $1/e^2$ widths of the intensity profiles in the beam waist and in the far-field. The experimental details of the set-up were discussed in detail by Hülsewede *et al.* (2001). For the devices under study the waist width and the far-field angle were measured at 25°C up to an output power of $P = 2$ W for the devices with $L_{RW} \leq 750$ μm and up to $P = 1.5$ W for the devices with $L_{RW} \geq 1000$ μm. Based on these data the beam propagation factor M^2 were calculated. The results for the lasers with the smallest M^2 for each geometry are compiled in the Fig. 2.

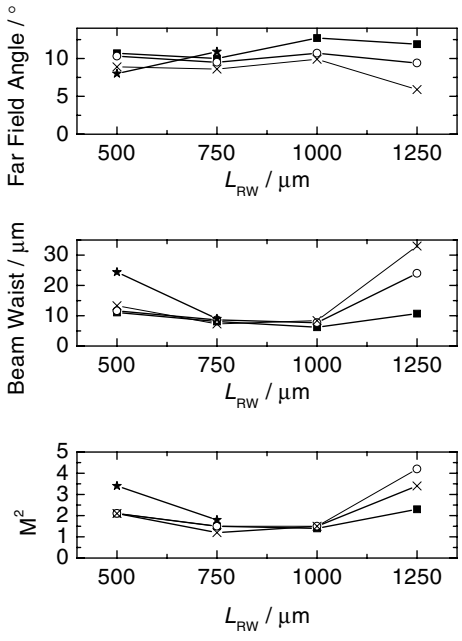

Fig. 2. Dependence of the best measured values for far-field angle (upper trace), the width of the beam waist (middle trace), and the beam propagation factor M^2 (lower trace) on the length of the RW L_{RW} for 2 mm long devices. The other parameters are the same like in Fig. 1. ■ – 500 mW, ○ – 1000 mW, × – 1500 mW, ★ – 2000 mW.

Up to a length $L_{RW} = 1000$ μm there are only minor changes in the far-field angle (top trace). At larger L_{RW}, there is a decrease of the far-field angle. Compared to the beam waist, the variation of the far-field angle is only small. The values between 8° and 13° are always below the maximum calculated value of 13.2° assuming an effective index of 3.3 and the given taper angle of 4°.

The width of the virtual beam waist (middle trace) shows a strong variation when changing the length of the RW. For all output powers the width of the beam waist decreases from $L_{RW} = 500$ to 750 μm. At output powers $P \leq 1.5$ W, the smallest beam waist were measured for $L_{RW} = 750$ and 1000 μm. For larger L_{RW} the beam waist width again increases for $L_{RW} = 1250$ μm.

The trend discussed for the beam waist is identical for the beam propagation factor M^2 (lower trace), i.e. for tapered lasers the decisive beam parameter is the width of the beam waist. The smallest $M^2 = 1.8$ for an output power $P = 2$ W was found if $L_{RW} = 750$ μm.

These trends are also valid taking into account all measured lasers (three lasers with $L_{RW} = 500$ μm, five lasers with $L_{RW} = 750$ μm, two devices with $L_{RW} = 1000$ μm, and one laser with $L_{RW} = 1250$ μm) and calculating the averaged values of the beam parameters (Fig. 3). For all output powers the

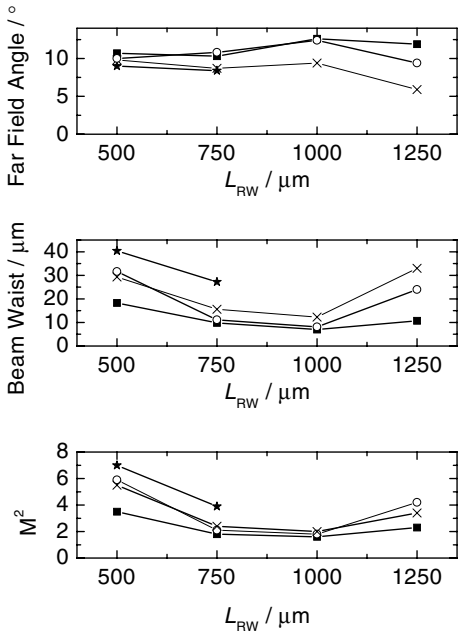

Fig. 3. Dependence of the averaged measured values for far-field angle (upper trace), the width of the beam waist (middle trace), and the beam propagation factor M^2 (lower trace) on the length of the RW L_{RW} for 2 mm long devices. The other parameters are the same like in Fig. 1. ■ – 500 mW, ○ – 1000 mW, × – 1500 mW, ★ – 2000 mW.

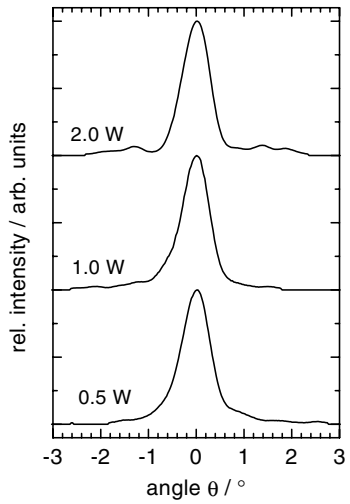

Fig. 4. Effective lateral far fields for a 2 mm long tapered diode laser with a length of the RW $L_{RW} = 750$ μm. The device parameters are same as Fig. 1.

far-field angle is nearly constant if $L_{RW} \leq 1000$ μm, whereas above this value the far-field becomes smaller. There is a minimum in the beam waist for $L_{RW} = 750$ and 1000 μm and for the same length a minimum for the beam propagation factor M^2 could also be observed.

Summarizing these results it could be stated that the optimum length of the RW was found to be $L_{RW} = 750$ μm for lasers with $L = 2$ mm, $\varphi_{TR} = 4°$, and $W_{RW} = 3$ μm. Here the highest output powers together with the best beam propagation factor could be measured. The lasers with $L_{RW} = 1000$ μm have also good beam parameters but suffer from a lower maximum output power.

The effective far-field for the laser with the best beam quality is shown in Fig. 4. From the plot it is obvious that the beam profile is nearly diffraction limited with only minor side lobes appearing at higher output powers. Up to the output power $P = 2$ W the $1/e^2$-width is smaller than 1.2°. For $P = 0.5$ W about 85% of the output power is concentrated in the central Gaussian lobe, at 1.0 W about 86% and at 2 W approximately 82%. Approximating a Gaussian shape for the central lobe and calculating the 4δ-width the central lobe has a width below 1.3°.

4. Characteristics of 4 mm long devices

The investigations made for the 2 mm long devices were also carried out for 4 mm long devices. Here the variations for the length of the RW were $L_{RW} = 500$, 1000, 1500 and 2000 μm.

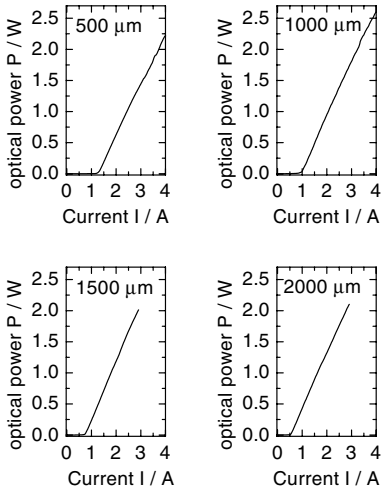

Fig. 5. Power–current characteristics for four tapered diode lasers with a total length $L = 4$ mm and different length of the RW L_{RW}. The other geometrical parameters are $\varphi_{TR} = 4°$ and $W_{RW} = 3$ µm. The measurement temperature was $T = 25°C$.

Table 2. Electro-optical parameter for tapered laser with a total length $L = 4$ mm and different L_{RW}

L_{RW} (µm)	I_{th} (mA)	S (W/A)	I_{max} (A)	P_{max} (I_{max}) (W)
500	1293	0.85	4.0	2.2
1000	977	0.90	4.0	2.6
1500	744	0.97	3.0	2.0
2000	538	0.92	3.0	2.2

The measured power–current characteristics are shown in Fig. 5, the electro-optical parameters compiled in Table 2. In any case a maximum output power $P \geq 2$ W was reached without failure of the diodes. The threshold current decreases as expected with increasing length of the RW. The slope efficiencies are in the range of 0.9 W/A. The wall-plug efficiencies for the diode with a shorter length of the RW were about 40%. The power current characteristics exhibit no kinks at all.

For four lasers, i.e. one of each geometry, the beam parameters were measured as described above. The measured data are compiled in Fig. 6.

In the top trace the dependence of the far-field on the length of the RW L_{RW} is plotted. Again a slight increase of the far-field angle with increasing L_{RW} could be stated. The far-field angle is smaller compared to the 2 mm long devices and covers the range between 7° and 10° ($1/e^2$-width). The variation is again small compared to the effect of the different L_{RW} on the beam waist. Whereas at smaller output powers all lasers have a small width of the beam waist (middle trace) below 20 µm and a beam quality parameter M^2 (lower trace) below three, at an output power $P = 2$ W a pronounced

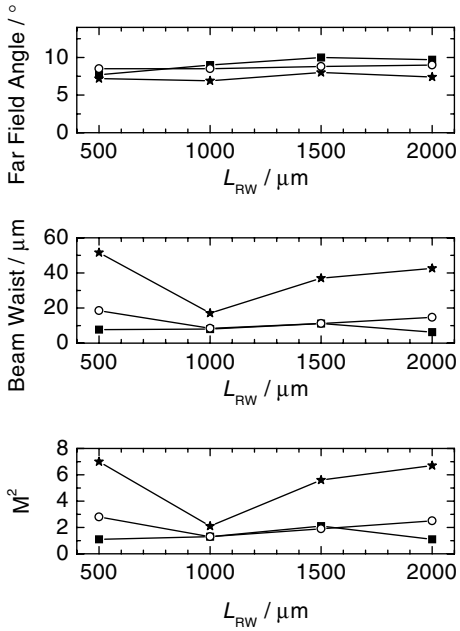

Fig. 6. Dependence of the measured values for far-field angle (upper trace), the width of the beam waist (middle trace), and the beam propagation factor M^2 (lower trace) on the length of the RW L_{RW} for 4 mm long devices. The other parameters are the same like in Fig. 5. ■ – 500 mW, ○ – 1000 mW, ★ – 2000 mW.

minimum in both plots can be seen. For 4 mm long lasers with $L_{RW} = 1000$ µm a beam propagation factor $M^2 = 2.1$ was measured.

Within the studied parameter set for this laser length $L = 4$ mm the optimal length of the RW L_{RW} is 1000 µm. For a laser with this geometry the effective far-field is plotted in Fig. 7. At output powers of 0.5 W and 1 W the effective far-field has one pronounced central lobe and only minor side lobes. About 80% for $P = 0.5$ W and 76% for $P = 1.0$ W of the output power are within the central lobe. At the higher output power $P = 2$ W the side lobes are much more pronounced and contain a considerable amount of energy. Therefore here only 59% of the output power is located in the central lobe. Measuring the $1/e^2$-width in all cases, the width is smaller than 0.45°. Approximating the central lobe by a Gaussian fit the 4δ-value is about 0.44° for $P = 0.5$ W and $P = 1.0$ W, but 0.55° for $P = 2$ W.

5. Discussion

For the 2 mm long devices, it is obvious that from the point of maximum output power the devices with smaller length of the RW section are preferable. Although the threshold current is higher compared to the devices with a larger L_{RW}, higher output powers were achieved due to the higher slope

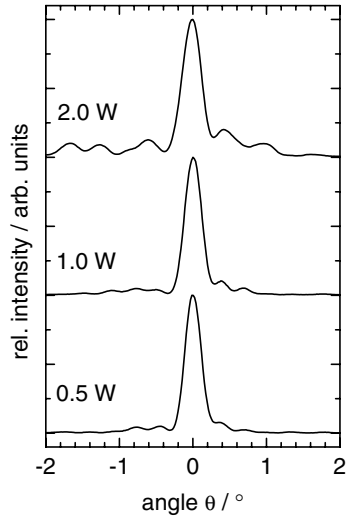

Fig. 7. Effective lateral far fields for a 4 mm long tapered diode laser with a length of the RW $L_{RW} = 1000$ μm. The device parameters are same as Fig. 5.

efficiency. This result is understandable: The devices with a short RW-section have the longest tapered section, which surely generates the majority of optical output power. A decrease of the length of the tapered section from 1500 μm down to 750 μm decreases also the output power by about a factor of two. For the lasers with the large L_{RW} the region for the gain is too small. In the tapered section the effect of self-focussing takes place. This fact could also be the reason for the failure of the lasers with $L_{RW} = 1250$ μm at excitation currents $I > 2$ A.

For the 4 mm long devices the higher output power was again measured for the devices with small L_{RW}-values. Nevertheless all devices reach an output power of 2 W. The tendency that the beam waist is quite large for the lasers with the shortest length of the RW $L_{RW} = 500$ μm for the 2 mm and the 4 mm long devices can be ascribed to the insufficient spatial mode filtering for these lasers. The length seems to be too short to suppress intensity of back-reflected light.

When increasing the length of the RW the filtering is more efficient and guarantees that in the waist position only a small area contributes to the laser emission. For an even longer ridge at constant total length, one can speculate that the RW is too strong excited and a broadening of the mode occurs. On the other hand at the same output power from the smaller aperture of the facet more light is back reflected into the taper. The ridge is not capable to filter all the backscattered light.

In any case, both for the power–current–characteristics and the beam parameter, the precise description would require a sophisticated three-di-

mensional theory including electronic, optical, and thermal effects in the system.

6. Conclusion

In conclusion, tapered diode lasers with a total length $L = 2$ and $L = 4$ mm were optimised concerning high-brightness at output power up to $P = 2$ W. With a non-sophisticated structure without any beam spoiling grooves, it was possible to obtain best beam propagation factors $M^2 \leq 2.1$. The tapered lasers consisted of an index-guided straight section and a gain-guided tapered region. The best geometries were:

- $L = 2$ mm, $L_{RW} = 750$ μm, $\varphi_{TR} = 4°$, $W_{RW} = 3$ μm with $M^2 = 1.8$ at P = 2 W, and
- $L = 4$ mm, $L_{RW} = 1000$ μm, $\varphi_{TR} = 4°$, $W_{RW} = 3$ μm with $M^2 = 2.1$ at P = 2 W.

Comparing the two total laser lengths, it is obvious that the 4 mm long lasers reach more easily higher output powers at acceptable beam quality. But the amount of energy in the central lobe is smaller compared to the 2 mm long lasers. The 2 mm long devices have in the case of $L_{RW} \leq 1000$ μm a good beam quality with a high content of power in the central lobe, but reach an output power $P = 2$ W only for $L_{RW} \leq 750$ μm. Therefore these results lead to the assumption that an intermediate laser length of about 2.5 mm and a length of a RW of 1000 μm could be a good compromise between the two above-mentioned optimised geometries. The excellent results for these devices with a record low $M^2 = 1.4$ at $P = 2$ W were published recently (Sumpf *et al.* 2002).

All these types of diode lasers are suitable tools for different medical applications, the pumping of solid-state lasers, and due to the small spectral bandwidth also for non-linear frequency conversion. Promising reliability test are in progress.

Acknowledgements

The authors acknowledge the support of this project by the European Community within the research project ULTRABRIGHT (IST-1999-10356). The authors wish to thank S. Sahre and P. Brade for the measurement of the samples.

References

Agahi, F., K.M. Lau, H.K. Choi, A. Baliga and N.G. Anderson. *IEEE Photon. Technol. Lett.* **7** 140, 1995.
Agahi, F., A. Baliga, K.M. Lau and N.G. Anderson. *Solid-State Electron.* **41** 647, 1997.
Al-Muhanna, A., J.K. Wade, L.J. Mawst and R.J. Fu. *Appl. Phys. Lett.* **72** 641, 1998a.

Al-Muhanna, A., J.K. Wade. T. Earles, J. Lopez and L.J. Mawst. *Appl. Phys. Lett.* **73** 2869, 1998b.
Bour, D.P., D.W. Treat, K.J. Beernink, R.L. Thornton, T.L. Paoli and R.D. Bringans. *IEEE Photon. Technol. Lett.* **6** 1283, 1994.
Donelly, J.P., J. Walpole, S.H. Groves, R.J. Bailey, L.J. Missaggia, A. Napoleone, R.E. Reeder and C.C. Cook. *IEEE Photonic. Technol. Lett.* **10** 1377, 1998.
Emanuel, M.A., J.A. Skidmore, M. Jansen and R. Nabiev. *IEEE Photon. Technol. Lett.* **9** 1451, 1997.
Erbert, G., F. Bugge, A. Knauer, J. Sebastian, A. Thies, H. Wenzel, M. Weyers and G. Tränkle. *IEEE J. Select. Topics Quantum Electron.* **5** 780, 1999.
Hülsewede, R., J. Sebastian, H. Wenzel, G. Beister, A. Knauer and G. Erbert. *Opt. Commun.* **192** 69, 2001.
Kintzer, E.S., J.N. Walpole, S.R. Chinn, C.A. Wang and L.J. Missaggia. *IEEE Photonic. Technol. Lett.* **5** 605, 1993.
Knauer, A., G. Erbert, H. Wenzel, A. Bhattacharya, F. Bugge, J. Maege, W. Pittroff and J. Sebastian. *Electron. Lett.* **35** 638, 1999.
Mikulla, M., P. Chazan, A. Schmitt, S. Morgott, A. Wetzel, M. Walther, R. Kiefer, W. Pletschen, J. Braunstein and G. Weimann. *IEEE Photonic. Technol. Lett.* **11** 654, 1998.
Pittroff, W., G. Erbert, G. Beister, F. Bugge, A. Klein, A. Knauer, J. Maege, P. Ressel, J. Sebastian, R. Staske and G. Tränkle. *IEEE Trans. Adv. Packaging* **24** 434, 2001.
Rusli, S., A. Al-Muhanna, T. Earles and L.J. Mawst. *Electron. Lett.* **36** 630, 2000.
Singh, R., D. Bull, F.P. Dabkowski, E. Clausen and A.K. Chin. *Appl. Phys. Lett.* **75** 2002, 1999.
Sumpf, B., G. Beister, G. Erbert, J. Fricke, A. Knauer, W. Pittroff, P. Ressel, J. Sebastian, H. Wenzel and G. Tränkle. *IEEE Photonic. Technol. Lett.* **13** 7, 2001a.
Sumpf, B., G. Beister, G. Erbert, J. Fricke, A. Knauer, W. Pittroff, P. Ressel, J. Sebastian, H. Wenzel and G. Tränkle. *Electron Lett.* **37** 351, 2001b.
Sumpf, B., R. Hülsewede, G. Erbert, C. Dzionk, J. Fricke, A. Knauer, W. Pittroff, P. Ressel, J. Sebastian, H. Wenzel and G. Tränkle. *Electron. Lett.* **38** 183, 2002.
Tihanyi, P.L., F.C. Jain, M.J. Robinson, J.E. Dixon, J.E. Williams, K. Meehan, M.S. O'Neill, L.S. Heath and D.M. Beyea. *IEEE Photon. Technol. Lett.* **6** 775, 1994.
Walpole, J.N. *Opt. Quantum Electron.* **28** 623, 1996.